Available online at www.sciencedirect.com
SCIENCE DIRECT®
Journal of Solid State Chemistry 177 (2004) 731–738
JOURNAL OF SOLID STATE CHEMISTRY
http://elsevier.com/locate/jssc

Synthesis and crystal structure of the $Sr_2MnGa(O,F)_6$ oxyfluorides

A.M. Alekseeva,[a] A.M. Abakumov,[a,*] M.G. Rozova,[a] E.V. Antipov,[a] and J. Hadermann[b]

[a] *Department of Chemistry, Moscow State University, Leninskie gory, Moscow 119992, Russia*
[b] *EMAT, University of Antwerp (RUCA), Groenenborgerlaan 171, B-2020 Antwerp, Belgium*

Received 11 August 2003; received in revised form 30 August 2003; accepted 3 September 2003

Abstract

The fluorine-containing derivatives of $Sr_2MnGaO_{5.5}$ were prepared by treatment with XeF_2 at temperatures ranging from 300°C to 600°C. The compounds crystallize in a tetragonal unit cell with $a_t \approx a_p$, $c_t \approx 2a_p$ (a_p—the parameter of the perovskite subcell). An increase in fluorine content is accompanied by a reduction of the Mn oxidation state due to a partial replacement of oxygen by fluorine. The crystal structure of $Sr_2MnGaO_{4.78}F_{1.22}$ was determined by electron diffraction and X-ray powder diffraction ($a = 3.85559(2)$ Å, $c = 7.78289(6)$ Å, S.G. $P4/mmm$, $R_I = 0.012$, $R_P = 0.019$). The structure consists of alternating (MnO_2), (SrO) and ($GaO_{0.78}F_{1.22}$) layers. The Ga atoms are situated in slightly elongated octahedra, the MnO_6 octahedra are characterized by two short apical Mn–O distances of 1.876(8) Å and four long equatorial ones of 1.9278(1) Å. This is interpreted as an "apically compressed" type of Jahn–Teller distortion, in contrast to the "apically elongated" one in the $Sr_2MnGaO_{5+\delta}$ brownmillerites with different oxygen content. Possible structural reasons for the reversed Jahn–Teller effect are discussed.

Keywords: $Sr_2MnGaO_{5-x}F_{1+x}$; Fluorination; Structure; X-ray diffraction; Electron diffraction

1. Introduction

$A_2MnGaO_{5+\delta}$ (A = Ca, Sr) brownmillerites [1–4] attract considerable attention due to a possible demonstration of the CMR effect, as was already found in $SrCaMnGaO_5$ [5]. The two-dimensional orthorhombically distorted structure ($a \approx c \approx \sqrt{2}a_p$, $b \approx 4a_p$) of these compounds is built up of layers of corner-sharing MnO_6 octahedra separated by zigzag chains of GaO_4 tetrahedra (Fig. 1). Recently, we have studied anion nonstoichiometry in $Sr_2MnGaO_{5+\delta}$ brownmillerite [6]. The oxygen content in $Sr_2MnGaO_{5+\delta}$ can be smoothly varied by annealings at partial oxygen pressure ranging from 10^{-5} to 1 atm. The increase of δ is accompanied by a gradual decrease of the orthorhombic distortion and symmetry changes from $Imma$ ($-0.03 \leqslant \delta \leqslant 0.13$, $a \approx c \approx \sqrt{2}a_p$, $b \approx 4a_p$, a_p—the parameter of the perovskite sublattice) to $Bmmm$ ($0.41 \leqslant \delta \leqslant 0.46$, $a \approx c \approx \sqrt{2}a_p$, $b \approx 2a_p$) and to tetragonal $P4/mmm$ ($\delta = 0.505$, $a \approx a_p$, $c \approx 2a_p$) [6]. In the compounds belonging to the low-oxidized region the MnO_6 octahedra are subjected to strong apical tension due to the Jahn–Teller effect inherent to Mn^{3+} cations. This distortion is gradually suppressed by increasing the Mn oxidation state which is reflected by the shortening of the apical Mn–O bond from 2.411(4) Å ($\delta = -0.03$) to 1.956(3) Å ($\delta = 0.5$). In the low-oxidized region the G-type magnetic structure is realized, in which the Mn magnetic moments are aligned normal to the (MnO_2) planes and are antiferromagnetically ordered along the [100], [010] and [001] directions of the perovskite subcell [4,7]. The insertion of extra oxygen atoms into the ($GaO_{1+\delta}$) layers changes the magnetic structure to the antiferromagnetic C-type, and the Mn magnetic moments become ordered antiferromagnetically within the (MnO_2) planes but the planes are ferromagnetically coupled. The transition from the G- to C-type magnetic structure by oxygen doping is explained by strong diagonal 180° superexchange antiferromagnetic interaction between Mn-ions in adjacent layers through additional oxygen atoms in the ($GaO_{1+\delta}$) buffer layer [7]. Thus, not only the electronic configuration of the Mn cations, but also the amount of anions in the Ga-layers and the coordination number of the Ga atoms appear to be important for the magnetic interactions in this material. An alternative way to vary

*Corresponding author. Fax: +95-939-47-88.
E-mail address: abakumov@icr.chem.msu.ru (A.M. Abakumov).

0022-4596/$ - see front matter © 2003 Elsevier Inc. All rights reserved.
doi:10.1016/j.jssc.2003.09.002

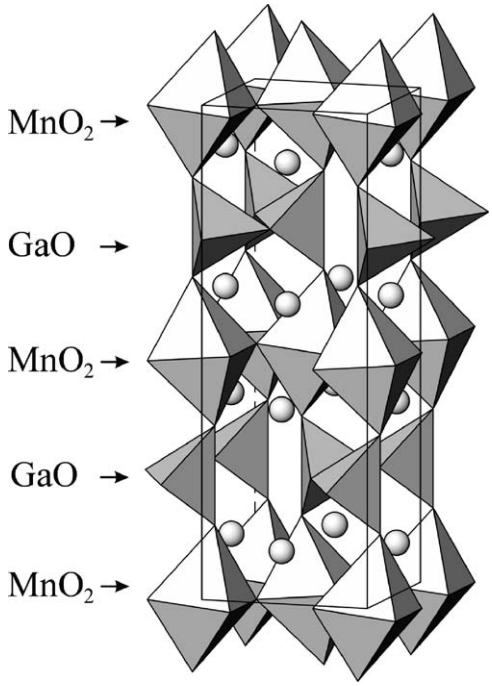

Fig. 1. Crystal structure of the Sr_2MnGaO_5 brownmillerite. The Mn atoms are situated in octahedra, the Ga atoms—in tetrahedra, Sr cations are shown as spheres. Ordered arrangement of the tetrahedral chains is shown for clarity.

the oxidation state of the Mn cations is an insertion of fluorine atoms into the Ga-layers with the formation of mixed Mn-based oxyfluorides. Due to the different formal charges of O^{2-} and F^-, different amounts of anions are required to create the same Mn oxidation state. This can alter the structure and properties of the oxyfluorides in comparison with the oxygen-doped compounds. Earlier we have demonstrated that fluorine atoms can be incorporated in the (GaO) layers of the $LaACuGaO_5$ (A = Ca, Sr) brownmillerites [8], and we can expect that the Mn-based brownmillerites can also be successfully fluorinated. In this contribution we describe the synthesis and structural features of the $Sr_2MnGaO_{5-x}F_{1+x}$ solid solutions prepared using XeF_2 as a fluorinating agent.

2. Experimental

The preparation of $Sr_2MnGaO_{5+\delta}$ with $\delta \approx 0$ was performed using a solid-state reaction in an evacuated sealed silica tube according to the procedure described in Ref. [2]. Part of the reduced phase was then oxidized by heating in oxygen flow at 400–415°C for 20–40 h to produce the material with $\delta \approx 0.5$. The prepared compounds were treated with XeF_2. The operations with XeF_2 were carried out in a glove box filled with dried N_2. 0.4 g of $Sr_2MnGaO_{5+\delta}$ was mixed with XeF_2 in molar ratios varying between 1:0.5 and 1:3 and ground in an agate mortar .The mixture was placed in a Ni crucible and sealed into an N_2-filled copper tube. The samples were annealed at temperatures ranging from 300°C to 600°C for 10–20 h and then furnace cooled to room temperature. The Mn formal valence (V_{Mn}) in the initial and fluorinated samples was determined by iodometric titration with a standard deviation of ± 0.03.

Phase analysis and measurements of cell parameters were performed using X-ray powder diffraction with a focusing Guinier-camera FR-552 (Cu$K\alpha_1$-radiation, Ge was used as an internal standard). X-ray powder diffraction data for crystal structure refinement were collected on an STADI-P diffractometer (Cu$K\alpha_1$-radiation, curved Ge monochromator, transmission mode, linear PSD). The RIETAN-2000 program was used for the Rietveld refinement [9]. Electron diffraction (ED) study was performed using Philips CM20 and JEM 2000FX2 transmission electron microscopes.

3. Results

3.1. Synthesis and characterization

The treatment of the reduced ($\delta \approx 0$) Sr_2MnGaO_5 phase ($a = 5.3959(7)$ Å, $b = 16.188(2)$ Å, $c = 5.5497(6)$ Å) with $XeF_2/Sr_2MnGaO_5 = 0.5{:}1$ molar ratio at 350°C results in a slight increase of the b parameter of the body-centered orthorhombic unit cell and in a decrease of orthorhombic distortion ($a = 5.3729(8)$ Å, $b = 16.233(7)$ Å, $c = 5.5053(7)$ Å). The latter is visible from comparing $(c-a)/(c+a)$ values, which are equal to 0.0141 and 0.0121 for the initial reduced and fluorinated samples, respectively. The oxidation state of Mn in this phase can be evaluated as $+3.20$ using the known V_{Mn} vs. b parameter dependence for the oxygen-doped $Sr_2MnGaO_{5+\delta}$ samples [6]. Further increase of the XeF_2/Sr_2MnGaO_5 ratio up to 3:1 and an increase of annealing temperature up to 400°C do not significantly change the cell parameters of the orthorhombic brownmillerite-type phase and result in the appearance of a new tetragonal phase. The reflections of this phase are indexed with cell parameters related to the cell parameters of the parent brownmillerite-type structure as $a_t \approx a_o/\sqrt{2}$, $c_t \approx b_o/2$ (subscript t stands for the tetragonal cell and subscript o for the orthorhombic one). The relative amount of the orthorhombic and tetragonal phases do not strongly depend on further increase of the fluorination temperature and the amount of XeF_2 in the starting mixture. Besides these phases, broad reflections corresponding to badly crystallized SrF_2 were observed on X-ray diffraction patterns that indicates a partial decomposition occurring simultaneously with the fluorination.

Because fluorination of the reduced Sr_2MnGaO_5 phase does not allow the preparation of single phase

Table 1
Fluorination conditions and cell parameters of initial and fluorinated compounds

#	Fluorination conditions	a (Å)	b (Å)	c (Å)	V_{Mn}
1	Initial I	5.381(1)	7.996(3)	5.360(1)	3.86
2	Initial II	3.8003(7)		7.948(3)	4.0
3	1:1 XeF_2, 300°C, 20 h	3.8265(9)		7.859(3)	
4	1:2 XeF_2, 400°C, 20 h	3.8486(1)		7.7886(2)	
5	1:1 XeF_2, 500°C, 10 h	3.8557(3)		7.7843(8)	3.78
6	1:1 XeF_2, 600°C, 20 h	3.865(1)		7.779(3)	3.54
7	1:3 XeF_2, 600°C, 20 h	3.8794(3)		7.7328(6)	3.39

samples with a wide range of fluorine contents, the interaction of the oxidized $Sr_2MnGaO_{5+\delta}$ ($\delta \approx 0.5$) sample with XeF_2 was investigated. Fluorination conditions, phase compositions, cell parameters and V_{Mn} for this series are listed in Table 1. Two initial compounds, the weakly orthorhombically distorted ($\delta \approx 0.43$, sample #1) and the tetragonal one ($\delta \approx 0.5$, sample #2) lead to similar results under the same fluorination conditions. The X-ray diffraction patterns of the fluorinated samples were indexed using a tetragonally distorted perovskite-based unit cell with $a_t \approx a_p$, $c_t \approx 2a_p$. It should be noted that the XRD pattern of sample #3 demonstrates a larger broadening of the $hk0$ reflections in comparison with neighboring reflections. This can either be related to a slight deviation from the tetragonal symmetry or to an inhomogeneity of the fluorine distribution in the sample. XRD patterns of the samples #3–7 exhibit broad peaks corresponding to badly crystallized SrF_2. The amount of SrF_2 impurity grows with increasing amount of XeF_2 and with the temperature of fluorination, as can be evaluated from the peak height of the strongest reflection of SrF_2 ($I_{rel} = 0.9\%$ for sample #5 and $I_{rel} = 8.2\%$ for sample #7). An increase of the fluorination temperature from 300°C to 600°C and a molar XeF_2/$Sr_2MnGaO_{5+\delta}$ ratio from 1 to 3 cause an increase of the a lattice parameter and a decrease of the c lattice parameter of the tetragonal phase (see Fig. 2). These changes occur simultaneously with a decrease of V_{Mn}. We should note, however, that iodometric titration only provides a rough estimate of the Mn formal valence for the tetragonal fluorinated phases in samples #6 and 7 because of the presence of impurity phases. The increasing a parameter and decreasing c parameter result in the lowering of the c/a ratio from 2.091 for the initial sample #2 to 1.993 for the sample #7. Due to this, the tetragonal splitting of the reflections is hardly observed on the XRD pattern of sample #7, as can be seen in Fig. 2 for the 1 1 0 and 1 0 2 reflections. However, the presence of weak 1 0 1 and 1 1 3/2 0 1 reflections suggests a tetragonal symmetry with $c_t \approx 2a_p$. Deviation from cubic symmetry becomes evident from an analysis of the FWHM vs. 2θ dependence. The $1\,1\,1_p = 1\,1\,2_t$ and

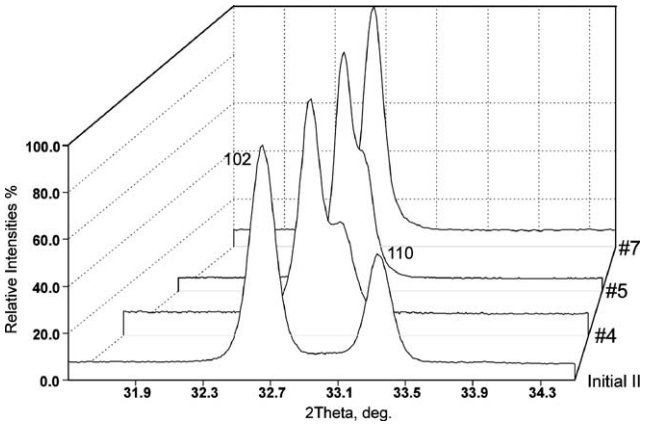

Fig. 2. Part of the XRD patterns of the initial $Sr_2MnGaO_{5.5}$ and fluorinated $Sr_2MnGaO_{5-x}F_{1+x}$ samples (#4, 5, 7) showing the positions of the 1 0 2 and 1 1 0 reflections. Note the decreasing splitting of 1 0 2 and 1 1 0 reflections upon increasing fluorine content on going from the initial sample to sample #7.

$2\,2\,2_p = 2\,2\,4_t$ reflections are less broadened in comparison with the neighboring reflections because they do not split on going from the cubic perovskite structure to the tetragonally distorted structure with $a_t \approx a_p$, $c_t \approx 2a_p$.

3.2. The crystal structure of $Sr_2MnGaO_{4.78}F_{1.22}$

The structure investigation was performed for the most pure sample #5, whose XRD pattern shows only traces of SrF_2. The reciprocal lattice of this compound was studied by electron diffraction. The most prominent ED patterns of $Sr_2MnGaO_{4.78}F_{1.22}$ are shown in Fig. 3. All reflections on the observed reciprocal lattice sections can be indexed on a tetragonal lattice with cell parameters as determined from XRD data. The spots on the $[001]^*$ pattern form a square arrangement, in agreement with the presence of a four-fold symmetry axis, and show an intensity distribution, characteristic for a perovskite structure. Doubling of the perovskite subcell parameter along the tetragonal c-axis becomes evident from the $0\,0\,l$, $l = 2n + 1$ spots, present on the $[100]^*$ and $[110]^*$ patterns. The absence of systematic extinctions was confirmed by tilting the crystals along the main reciprocal lattice axes. This suggests $P4/mmm$ as the most symmetric space group for this compound. The compound appears to be stable only under a spread electron beam, as used for selected area electron diffraction. Being irradiated by an intense focused beam, needed for recording high-resolution electron microscopy images, the compound immediately decomposes, which hinders the HREM investigation of this material.

The fluorinated phase of sample #7 was also studied using electron diffraction. The electron diffraction patterns of the $[001]^*$, $[100]^*$ and $[110]^*$ zones are essentially the same as those observed for

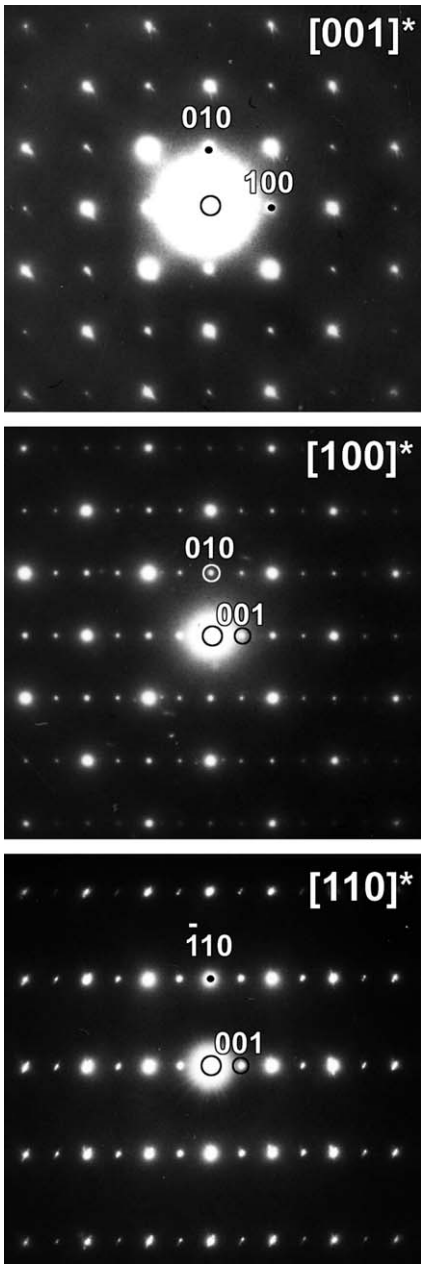

Fig. 3. ED patterns of $Sr_2MnGaO_{4.78}F_{1.22}$ sample (#5).

$Sr_2MnGaO_{4.78}F_{1.22}$ (Fig. 3) which confirms the tetragonally distorted $a_t \approx a_p$, $c_t \approx 2a_p$ unit cell.

Since no extinctions were observed on neither the XRD nor the ED patterns of the $Sr_2MnGaO_{4.78}F_{1.22}$ phase, the $P4/mmm$ space group was chosen to build a starting structure model for the Rietveld refinement. The atomic coordinates were transformed from a perovskite structure and full occupancy was assigned to all anion positions giving the $Sr_2MnGa(O,F)_6$ composition. Since oxygen and fluorine atoms have close scattering powers they were refined with oxygen scattering factors. To take into account the small broad peaks of SrF_2, it was introduced as a second phase into the refinement. In order to check the presence of anion vacancies, the occupancy factors of the O(1), O(2) and O(3) positions were refined with a fixed atomic displacement parameter $B = 0.5\,Å^2$. The refined occupancies $g\mathrm{O}(1) = 1.07(1)$, $g\mathrm{O}(2) = 0.99(1)$, $g\mathrm{O}(3) = 0.993(7)$ show that all anion positions are fully occupied. For the final refinement the occupancy factors for the anions were fixed to 1. The refinement was performed with an isotropic approximation for the atomic displacement parameters, which were refined independently for each atomic position. Excellent values of reliability factors ($R_I = 0.012$, $R_P = 0.019$) indicate a good agreement between experimental and calculated profiles (Fig. 4). The crystallographic parameters, reliability factors, atomic coordinates and the most relevant interatomic distances for $Sr_2Mn(O,F)_6$ are listed in Tables 2–4.

Since subtle structure distortions are very common in perovskites, we have analyzed the X-ray diffraction profile of the sample #5 in details. FWHM vs. 2θ dependence was found to be non-monotonic: the 1 1 2,

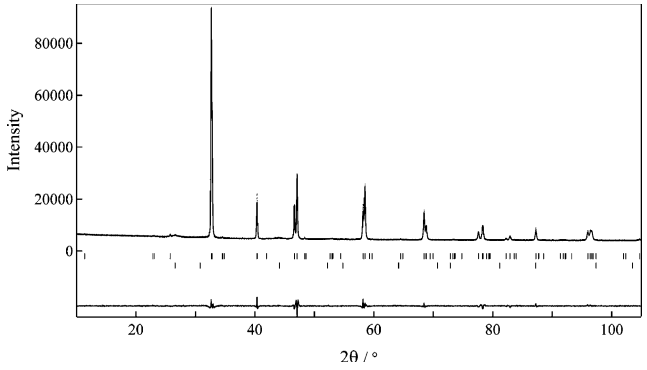

Fig. 4. Experimental, calculated and different X-ray diffraction profiles for $Sr_2MnGaO_{4.78}F_{1.22}$. Upper and lower tick rows mark the position of reflections belonging to $Sr_2MnGaO_{4.78}F_{1.22}$ and SrF_2, respectively.

Table 2
Selected parameters from Rietveld refinement of X-ray powder data for $Sr_2MnGaO_{4.78}F_{1.22}$

	$Sr_2MnGaO_{4.78}F_{1.22}$
Space group	*P4/mmm*
a (Å)	3.85559(2)
c (Å)	7.78289(6)
Z	1
Cell volume (Å^3)	115.697(1)
Calculated density (g/cm^3)	5.682
2θ range, step (deg)	$10 \leqslant 2\theta \leqslant 105$, 0.01
Number of reflections	59
Refinable atomic parameters	9
Reliability factors	
R_P, R_{wP}	0.019, 0.031
R_I ($Sr_2MnGaO_{4.78}F_{1.22}$)	0.012
R_I (SrF_2)	0.008
Mass fraction in the sample	
$Sr_2MnGaO_{4.78}F_{1.22}/SrF_2$	0.94/0.06

Table 3
Positional and thermal parameters of atoms for $Sr_2MnGaO_{4.78}F_{1.22}$

Atom	Position	x/a	y/b	z/c	B_{iso} (Å)^2
Sr	2*h*	1/2	1/2	0.2460(4)	0.32(2)
Mn	1*b*	0	0	0	1.6(1)
Ga	1*a*	0	0	1/2	0.9(1)
O(1)	2*e*	1/2	0	0	0.1(3)
O(2)[a]	2*g*	1/2	0	1/2	0.7(3)
O(3)	2*f*	0	0	0.2410(5)	0.5(1)

[a]The position is occupied together by oxygen and fluorine: 0.61F + 0.39O.

Table 4
Selected interatomic distances for $Sr_2MnGaO_{4.78}F_{1.22}$ (Å)

Sr–O(1)	2.717(2) × 4
Sr–O(2)	2.7266(1) × 4
Sr–O(3)	2.761(2) × 4
Mn–O(1)	1.9278(1) × 4
Mn–O(3)	1.876(8) × 2
Ga–O(2)	1.9278(1) × 4
Ga–O(3)	2.016(8) × 2

1 1 4 and 2 2 4 reflections are less broadened than the reflections from the same 2θ regions (that is not the case, however, for the 1 1 0, 2 2 0 and 0 0 4 reflections). At the same time the 2 0 0, 3 0 2, 3 1 0 and 3 1 2 reflections have larger FWHMs. An attempt was made to describe this observation with the orthorhombic *Pmmm* model with $a \approx b \approx a_p$, $c \approx 2c_p$ since it is compatible with the electron diffraction data if one takes into account small difference between a and b. The Rietveld refinement gave slightly different a and b cell parameters ($a = 3.85958(3)$ Å, $b = 3.85165(3)$ Å, $c = 7.78309(5)$ Å) and only minor improvement of profile description ($R_P = 0.017$). Atomic coordinates obtained after the refinement of the *Pmmm* model are indentical to those in the $P4/mmm$ structure in the range of two standard deviations. Therefore, we should conclude that the conventional X-ray powder pattern does not provide solid arguments for breaking down the tetragonal symmetry, and the data on the $Sr_2MnGaO_{4.78}F_{1.22}$ crystal structure are discussed further assuming the $P4/mmm$ symmetry.

Further details of the crystal structure investigation can be obtained from the Fachinformationszentrum Karlsruhe, 76344 Eggenstein-Leopoldshafen, Germany (fax: +49-7247-808-666; mailto:crysdata@fiz.karlsruhe.de) on quoting the depository number CSD 413076.

The main difference between the oxygen-doped $Sr_2MnGaO_{5.5}$ phase and the fluorinated $Sr_2MnGaO_{4.78}F_{1.22}$ phase is the full occupation of the anion positions in the latter structure with a formation of an octahedral environment around the Ga atoms. The reasonably low atomic displacement parameter for the Ga atom

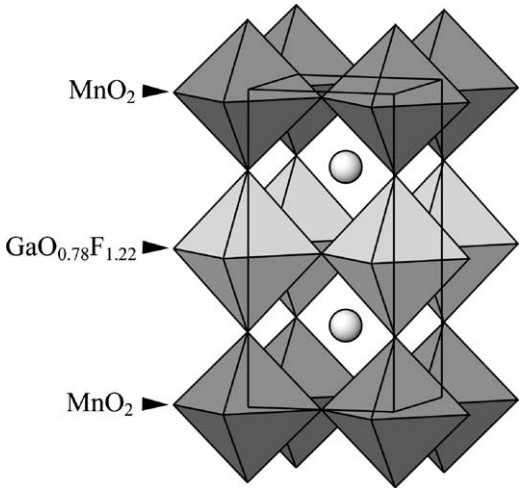

Fig. 5. Crystal structure of $Sr_2MnGaO_{4.78}F_{1.22}$ MnO_6 octahedra are darker shaded.

($B = 0.9(1)$ Å^2) supports a complete octahedral coordination for these cations. This value can be compared with that in the $Sr_2MnGaO_{5.5}$ structure, where the large $B(Ga) = 3.7(1)$ Å^2 reflects a static disorder due to the incomplete coordination of Ga by oxygen atoms. The Mn formal valence $V_{Mn} = +3.78$ known from iodometric titration allows to calculate the relative amounts of oxygen and fluorine and propose the $Sr_2MnGaO_{4.78}F_{1.22}$ formula for the fluorinated phase in the sample #5.

In the $Sr_2MnGaO_{4.78}F_{1.22}$ crystal structure the Mn and Ga atoms are situated in slightly distorted octahedra (Fig. 5). From the X-ray diffraction experiment the positions of fluorine and oxygen can not be distinguished. However, the bond valence sum (BVS) calculations performed on a base of the obtained interatomic distances strongly support the location of fluorine in the $\frac{1}{2},0,\frac{1}{2}$ position, i.e. in the equatorial environment of the Ga atoms. The details of the BVS calculations are given below. The octahedral environment around the Mn atoms can be described as "apically compressed" with two short apical Mn–O distances of 1.876(8) Å and four long equatorial ones of 1.9278(1) Å. At the same time the octahedron around the Ga atoms is characterized by two apical Ga–O distances of 2.016(8)Å, which are longer than four equatorial Ga–(O,F) ones. The average interatomic distances are $\langle d(Mn-O)\rangle = 1.911$ Å and $\langle d(Ga-(O,F))\rangle = 1.957$ Å. These values agree well with the sum of the corresponding ionic radii calculated as weighed averages taking into account a common occupation of the 0,0,0 postion by Mn^{3+} and Mn^{4+} and the $\frac{1}{2},0,\frac{1}{2}$ position by O^{2-} and F^- according to the proposed compound stoichiometry ($\langle d(Mn-O)\rangle = 0.78r(Mn^{4+}) + 0.22r(Mn^{3+}) + r(O^{2-}) = 1.91$ Å, $\langle d(Ga-(O,F))\rangle = r(Ga^{3+}) + 0.59r(O^{2-}) + 0.41r(F^-) = 1.95$ Å, $r(Mn^{4+}) =$

0.68 Å, $r(Mn^{3+}) = 0.79$ Å, $r(Ga^{3+}) = 0.76$ Å (CN = 6), $r(O^{2-}) = 1.21$ Å, $r(F^{-}) = 1.15$ Å (CN = 2)).

The distribution of oxygen and fluorine atoms was evaluated using BVS calculations. The average Ga formal valence was calculated as a sum over the first coordination sphere of bond valences taken as $\exp[(R_0 - R)/B]$ with $R_0 = 1.730$ Å, $B = 0.37$ Å [10] for three different limiting cases:

(1) Ga is surrounded by oxygen atoms only.
(2) $Ga(O_4^{eq}F_2^{ap})$ and $Ga(O_4^{eq}O_1^{ap}F_1^{ap})$ octahedra are intermixed in the structure with the 0.22:0.78 ratio as required by the fluorine to oxygen ratio.
(3) $Ga(F_3^{eq}O_1^{eq}O_2^{ap})$ and $Ga(F_2^{eq}O_2^{eq}O_2^{ap})$ octahedra are intermixed in the structure with the 0.44:0.56 ratio as required by the fluorine to oxygen ratio.

In case 3, where all fluorine atoms are located in the equatorial plane of the $Ga(O,F)_6$ octahedron, a BVS value of +3.01 was obtained. The cases 1 and 2 give BVS values of +3.27 and +3.17, respectively, which are far from the Ga valence of +3. This result suggests the location of F atoms in the $\frac{1}{2},0,\frac{1}{2}$ position, and no significant replacement of oxygen by fluorine in the MnO_6 octahedra. The BVS value for the Mn cations was calculated as +3.72, which is close to the experimentally determined value of $V_{Mn} = +3.78$. For this calculation the R_0 value was taken as a weighed average of $R_0(Mn^{4+}) = 1.725$ Å and $R_0(Mn^{3+}) = 1.760$ Å. Instead of the tabulated $R_0(Mn^{4+}) = 1.753$ Å value the $R_0(Mn^{4+}) = 1.725$ Å constant was used, which was proven to give reliable results for nearly stoichiometric $SrMnO_{3-\delta}$ and $La_{0.85}Ca_{0.15}MnO_3$ [11].

The location of fluorine atoms predominantly at the $\frac{1}{2},0,\frac{1}{2}$ position can also be supported by comparing the lattice energies, calculated for a placement of fluorine in three different positions—$\frac{1}{2}$,0,0, $\frac{1}{2}$,0,$\frac{1}{2}$ and 0,0,0.24. For all cases the Madelung constant computations were made using the Ewald method [12]. The atomic coordinates were taken from the $Sr_2MnGaO_{4.78}F_{1.22}$ crystal structure, the charges were calculated as a weighed average of the formal charges, where the occupancy factors were taken as the weight factors. A placement of fluorine atoms in the $\frac{1}{2},0,\frac{1}{2}$ position provides an energy gain of 372 and 1407 kJ/mol compared with the cases where the fluorine atoms are located at the $\frac{1}{2}$,0,0 and 0,0,0.24 positions, respectively.

An attempt was made to refine the structure of the phase obtained by fluorination at 600°C for 20 h with $XeF_2/Sr_2MnGaO_{5+\delta} = 3{:}1$ (sample #7) using the structure model determined for $Sr_2MnGaO_{4.78}F_{1.22}$. However, in spite of good reliability factors ($R_I = 0.020$, $R_P = 0.028$), the accuracy of the Rietveld refinement was significantly lowered due to the large amount of badly crystallized SrF_2 admixture and a strong overlap of the reflections due to close a_t and $c_t/2$ values. In comparison with the $Sr_2MnGaO_{4.78}F_{1.22}$ structure the reduction up to $V_{Mn} = +3.39$ is accompanied by a further shortening of the Mn–O_{ap} distance (1.85(3) Å) and an increase of the Mn–O_{eq} and Ga–$(O,F)_{eq}$ ones (1.9411(1) Å) whereas $d(Ga–O_{ap}) = 2.02(3)$ Å bond distance does not change. However, since the value of V_{Mn} for this sample can be only roughly estimated by chemical analysis and the interatomic distances were determined with rather large standard deviations, we avoid a detailed interpretation of the relation between V_{Mn} and the interatomic distances.

4. Discussion

Strongly reduced ($\delta \approx 0$) and strongly oxidized ($\delta \approx 0.5$) $Sr_2MnGaO_{5+\delta}$ phases behave differently in the reaction with XeF_2. The fluorination of the reduced material at 350°C results in an increase of V_{Mn} and occurs mostly as a fluorine insertion. This process requires rather low fluorination temperature (below 400°C) to avoid a competing reaction of anion exchange which dominants usually at $t > 400$°C [13] and has a reductive character. Low fluorination temperature can cause kinetic difficulties explaining low amount of fluorine incorporating into the reduced Sr_2MnGaO_5 phase (about ~0.2F per formula unit). Insertion of fluorine at these conditions does not significantly alter the brownmillerite structure except for a small variation of the cell parameters, which is very similar to that observed previously for oxygen insertion [6]. The structural reasons for these changes upon increasing the amount of anions in the ($GaO_{1+\delta}$) layer were already discussed in detail in Ref. [6,8]. Increasing the temperature of the fluorination results in the formation of two fluorinated phases with perovskite-based structures, which probably differ by fluorine content due to a competition between fluorine insertion and anion exchange reactions. An inhomogeneous fluorination is a known phenomenon in the non-equilibrium fluorination process, as was often observed for fluorinated mixed copper-based oxides [13].

The known formal oxidation state of the Mn cations and the results of the refinement of the $Sr_2MnGaO_{4.78}F_{1.22}$ crystal structure allow us to propose a possible scheme for the fluorination of the compound with $\delta \approx 0.5$. Fluorine occupies all vacant anion sites in the ($GaO_{1.5}$) layers resulting in the $Sr_2MnGa(O,F)_6$ composition. The results of the iodometric titration show that formal Mn valence decreases with increasing temperature of fluorination and $XeF_2/Sr_2MnGaO_{5.5}$ molar ratio in the starting mixture. It suggests that a reductive reaction of partial replacement of oxygen by fluorine in the Ga-layers takes place. One can assume that the fluorination reaction at the experimental conditions close to those used for preparation of $Sr_2MnGaO_{4.78}F_{1.22}$ compound ($t = 500-600$°C, time

10–20 h) would occur according to the same possible overall scheme, which can be suggested as follows:

$$Sr_2MnGaO_{5.5} + (1+x)/2XeF_2 \rightarrow Sr_2MnGaO_{5-x}F_{1+x} + (0.5+x)[O] + (1+x)/2Xe.$$

Oxygen atoms released in this reaction are absorbed at the inner walls of the copper tube. An evaluation of the partial oxygen pressure inside the copper tube at the conditions of fluorination is given in Ref. [13]. Increasing the temperature of the fluorination and the amount of XeF_2 increases the degree of the anion replacement resulting in a gradual decrease of the formal Mn valence in the samples #5–7.

It is interesting to compare the behavior of oxygen-doped $Sr_2MnGaO_{5+\delta}$ and fluorine doped compounds upon variation of the Mn oxidation state. In both cases the equatorial Mn–O distances in the MnO_6 octahedra increases simultaneously with decreasing V_{Mn} (decreasing δ or increasing F content): from 1.9001 Å for $V_{Mn} = +4$ to 1.9222 Å ($V_{Mn} = +3.26$, $\delta = 0.13$) [6] and 1.9411 Å ($V_{Mn} = +3.39$, $x_F = 0.61$, an estimation). These changes follow an increase of the Mn cation size upon reduction. However, the apical Mn–O distance varies differently in the $Sr_2MnGaO_{5-x}F_{1+x}$ solid solutions in comparison to that in the $Sr_2MnGaO_{5+\delta}$ ones. Elongation of the Mn–O_{ap} distance occurs together with a decrease of δ for the $Sr_2MnGaO_{5+\delta}$ compounds due to an increase of the degree of Jahn–Teller distortion: 1.956(3) Å ($\delta = 0.5$), 1.983(6) Å ($\delta = 0.46$), 2.225(8) Å ($\delta = 0.13$), 2.372(5) Å ($\delta = 0.025$) and 2.411(4) Å ($\delta = -0.03$) [6]. For the $Sr_2MnGaO_{5-x}F_{1+x}$ solid solutions the c lattice parameter decreases together with decreasing V_{Mn} which may indicate a progressive apical compression of the MnO_6 octahedra. Indeed, d(Mn–O_{ap}) = 1.876(8) Å in the $Sr_2MnGaO_{4.78}F_{1.22}$ and d(Mn–O_{ap}) = 1.853(29) Å in the sample #7 are clearly shorter than d(Mn–O_{ap}) = 1.956(3) Å in $Sr_2MnGaO_{5.5}$ [7]. At the same time, the apical Ga–O distance stays the same for all structures within the range of standard deviations: 2.024(3) Å for $Sr_2MnGaO_{5.5}$ [7], 2.016(8) Å for $Sr_2MnGaO_{4.78}F_{1.22}$ and 2.02(3) Å for sample #7. It confirms that the compression of the unit cell of the $Sr_2MnGaO_{5-x}F_{1+x}$ solid solutions along the c-axis occurs due to a shortening of the Mn–O_{ap} bonds. Thus, we can propose that the reduction of V_{Mn} by fluorination reverses the type of Jahn–Teller distortion of the MnO_6 octahedra from "apically elongated" to "apically compessed".

We assume that the reversed Jahn–Teller effect in the fluorinated samples arises from an interplay between the decrease of the free energy from a stabilization due to a Jahn–Teller distortion and a simultaneous variation of the electrostatic lattice energy due to changes in the bond distances. In the oxygen doped $Sr_2MnGaO_{5+\delta}$ compounds the increase of the apical elongation of the MnO_6 octahedra is to some degree compensated by the decrease of Ga–O_{ap} distance due to a decrease of the coordination of Ga down to 4 [6]. For the $Sr_2MnGaO_{5-x}F_{1+x}$ solid solutions the Ga–O_{ap} distance does not alter since no changes in the coordination number occur and the average ionic radius of the apical anions does not change (all fluorine atoms are concentrated at the equatorial positions). Thus, if the reduction of the Mn cations will be accompanied by an elongation of the Mn–O_{ap} distances, it will result in abnormally long Sr–O separations and in a decrease of the lattice energy. We performed an evaluation of the lattice energy for two types of the $Sr_2MnGaO_{5-x}F_{1+x}$ solid solutions:

I. When the increase of the fluorine content is accompanied by shortening the Mn–O_{ap} distances (as experimentally observed).

II. When considering a hypothetical structure with elongation of the Mn–O_{ap} distances.

A number of extrapolations should be made to get the structural data for these calculations. The V_{Mn} vs. a parameter dependence was approximated using four experimentally known points for the $Sr_2MnGaO_{5-x}F_{1+x}$ solid solutions (samples #2, 5, 6, 7) that gave a linear equation $V_{Mn} = 31.5 - 7.2a$. From this equation V_{Mn} and the fluorine content for the samples #3 and 4 were calculated which allowed to assign formal charges for the atoms in all points of the solid solution assuming the fluorine atoms to be located at $\frac{1}{2},0,\frac{1}{2}$ position. The z coordinate of the O(3) atom was calculated for the cases I and II from the constant Ga–O_{ap} distance of 2.016 Å. In case II the Mn–O_{ap} distance was evaluated from the structural data measured on the oxygen doped $Sr_2MnGaO_{5+\delta}$ samples [6] (d(Mn–O_{ap}) = 3.66–0.43V_{Mn}, where V_{Mn} was evaluated as described above). From the sum of d(Ga–O_{ap}) = 2.016 Å and d(Mn–O_{ap}) the c parameter for the series II was calculated. It increases from $c = 7.948$ Å for $V_{Mn} = +4.0$ to $c = 8.454$ Å for $V_{Mn} = +3.39$. The lattice energy vs. V_{Mn} plot for both cases is presented in Fig. 6. It can be seen that a decreasing V_{Mn} results in an increasing gain of the lattice energy for the solid solutions I in comparison with the solid solutions II, which achieves ~1000 kJ/mol at $V_{Mn} = +3.39$. From the crystal field theory, for a high-spin d^4 electronic configuration apically elongated and apically compressed octahedra are energetically equivalent, but the latter in the $Sr_2MnGaO_{5-x}F_{1+x}$ structure provides an additional stabilization due to the gain in the electrostatic energy.

It is interesting to compare the coordination environment of Mn cations in oxygenated $Sr_2MnGaO_{5.5}$, fluorinated $Sr_2MnGaO_{4.78}F_{1.22}$ compounds and the solid solutions $Nd_{1-x}Sr_xMnO_3$ ($0.51 < x < 0.8$). At low temperature for $x = 0.63$ a tetragonal perovskite structure was found exhibiting C-type insulating antiferromagnetism. MnO_6 octahedra in this structure are apically elongated (d(Mn–O_{ap}) = 1.967 Å, d(Mn–O_{eq}) = 1.901 Å at $T = 10$ K) and the magnetic structure was

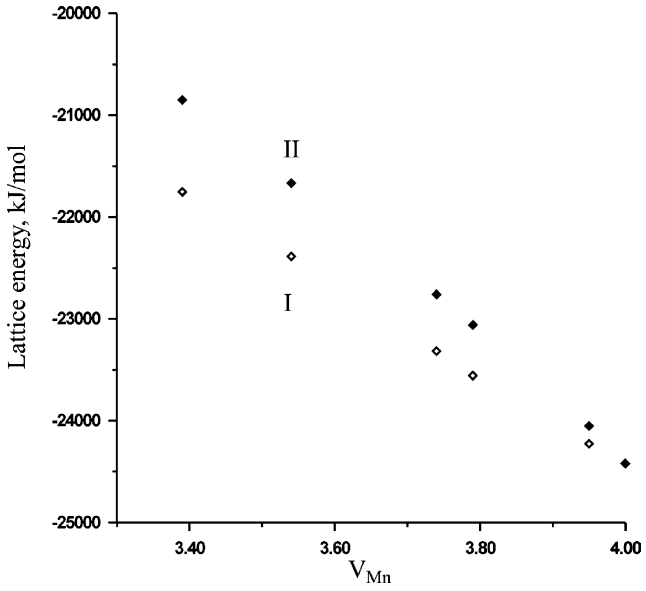

Fig. 6. Lattice energy vs. V_{Mn} dependencies calculated for the apical compression (I, open squares) and "apical elongation" (II, black squares) of the MnO_6 octahedar.

interpreted as driven by Mn $d_{3z^2-r^2}$ orbital ordering [14]. Decreasing x down to 0.55 results in an orthorhombically distorted perovskite structure. A characteristic feature of this structure is an "apical compression" of MnO_6 octahedra (d(Mn–O_{ap}) = 1.896 Å, d(Mn–O_{eq}) = 1.941 Å at $T = 15$ K) that was related to a planar $d_{x^2-y^2}$ orbital ordering resulting in metallic A-type antiferromagnetism [14]. A reversed distortion of the MnO_6 octahedra in $Sr_2MnGaO_{4.78}F_{1.22}$ can also lead to drastic changes in the magnetic structure and transport properties in comparison with the oxygen-doped $Sr_2MnGaO_{5.5}$ sample. Low temperature neutron diffraction experiments are in progress to reveal possible changes in the magnetic structure caused by fluorination.

Acknowledgments

The American Chemical Society Petroleum Research Fund is acknowledged for partial support of this research (project 38459-AC5). This work was supported in part by the program IAP V−1 of the Belgium government. A.M.A. is grateful to the INTAS for the Fellowship grant for Young Scientists YSF 2002-48. E.V.A. is grateful to Russian Science Support Foundation for the financial support. Authors are grateful to Dr. A. Knot'ko for the help with the electron microscopy investigation.

References

[1] A.M. Abakumov, M.G. Rozova, B.Ph. Pavlyuk, M.V. Lobanov, E.V. Antipov, O.I. Lebedev, G. Van Tendeloo, D.V. Sheptyakov, A.M. Balagurov, F. Bouree, J. Solid State Chem. 158 (2001) 100.
[2] A.M. Abakumov, M.G. Rozova, B.Ph. Pavlyuk, M.V. Lobanov, E.V. Antipov, O.I. Lebedev, G. Van Tendeloo, O.L. Ignatchik, E.A. Ovtchenkov, Yu.A. Koksharov, A.N. Vasi'ev, J. Solid State Chem. 160 (2001) 353.
[3] A.J. Wright, H.M. Palmer, P.A. Anderson, C. Greaves, J. Mater. Chem. 11 (2001) 1324.
[4] A.J. Wright, H.M. Palmer, P.A. Anderson, C. Greaves, J. Mater. Chem. 12 (2002) 978.
[5] P.D. Battle, A.M. Bell, S.J. Blundell, A.I. Coldea, D.J. Gallon, F.L. Pratt, M.J. Rosseinsky, C.A. Steer, J. Solid State Chem. 167 (2002) 188–195.
[6] A.M. Abakumov, M.G. Rozova, A.M. Alekseeva, M.L. Kovba, E.V. Antipov, O.I. Lebedev, G. Van Tendeloo, Solid State Sci. 5 (2003) 871–882.
[7] V.Yu. Pomjakushin, A.M. Balagurov, T.V. Elzhov, D.V. Sheptyakov, P. Fisher, D.I. Khomskii, V.Yu. Yushankhai, A.M. Abakumov, M.G. Rozova, E.V. Antipov, M.V. Lobanov, S.J.L. Billinge, Phys. Rev. B 66 (2002) 184412.
[8] J. Hadermann, G. Van Tendeloo, A.M. Abakumov, B.Ph. Pavlyuk, M. Rozova, E.V. Antipov, Int. J. Inorg. Mater. 2 (2000) 493.
[9] F. Izumi, T. Ikeda, Mater. Sci. Forum 198 (2000) 321.
[10] I.D. Brown, D. Altermatt, Acta Crystallogr. Sect. B: Struct. Sci. 41 (1985) 244.
[11] M.V. Lobanov, A.M. Balagurov, V.Ju. Pomjakushin, P. Fisher, M. Gutmann, A.M. Abakumov, O.G. D'yachenko, E.V. Antipov, O.I. Lebedev, G. Van Tendeloo, Phys. Rev. B 61 (2000) 8941.
[12] S.G. Popov, V.A. Levitskiy, Zh. Fiz. Khim. LV (1981) 87 (Russia).
[13] A.M. Abakumov, M.G. Rozova, E.I. Ardashnikova, E.V. Antipov, Russ. Chem. Rev. 71 (2002) 383.
[14] R. Kajimoto, H. Yoshizawa, H. Kawano, H. Kuwahara, Y. Tokura, K. Ohoyama, M. Ohashi, Phys. Rev. B 60 (1999) 9506.